Cell culture experiments

Gastric cancer cell lines, MKN45, MKN74 and Kato-III (Riken Bioresource Center, Tsukuba, Japan) were cultured in RPMI1640 or DMEM supplemented with 10% fetal bovine serum. Knockdown experiments were performed using Silencer Select Pre-designed siRNA and negative control siRNA (Life Technologies, Carlsbad, CA, USA). For the soft agar proliferation/colony formation assay, cells were mixed in 0.4% agar and seeded in a 96-well or six-well plate and cultured for 1 or 3 weeks, respectively. Then, 96-well plates were stained with AlamarBlue reagent (Life Technologies), and the fluorescence intensity was measured to examine the cell number. Six-well plates were stained with Giemsa solution (Wako, Osaka, Japan) and colony numbers were scored. For the sphere formation assay, MKN74 cells were plated in ultra-low attachment plates (Corning, Corning, NY, USA) and were cultured under hypoxic conditions at 3% O_2 and 5% CO_2. After 10 days, the number of spheres was counted.

The primary culture of gastric epithelial cells was described previously.[45] Briefly, mouse glandular stomachs were treated with 0.1% collagenase, followed by centrifugation at 20 *g* for 3 min to isolate gastric glands. Isolated glands were digested with trypsin and cultured on collagen-coated dishes. On day 2, the cells were passaged to induce differentiation. The primary cultured cells on day 2 and day 6 were used as undifferentiated and differentiated gastric epithelial cells, respectively.

Statistical analysis

The data were analyzed using the unpaired *t*-test and are presented as the means ± s.d. A value of $P<0.05$ was considered to be statistically significant.

CONFLICT OF INTEREST

The authors declare no conflict of interest.

ACKNOWLEDGEMENTS

We thank Manami Watanabe and Ayako Tsuda for their excellent technical assistance. This work was supported by Grants-in-Aid for Scientific Research on Innovative Areas (no. 22114005) from the Ministry of Education, Culture, Sports, Science and Technology of Japan; and CREST, the Japan Science and Technology Agency, Japan.

REFERENCES

1 Parkin DM, Bray F, Ferlay J, Pisani P. Global cancer statistics, 2002. *CA Cancer J Clin* 2005; **55**: 74–108.
2 Peek Jr RM, Blaser MJ. *Helicobacter pylori* and gastrointestinal tract adenocarcinomas. *Nat Rev Cancer* 2002; **2**: 28–37.
3 Fox JG, Wang TC. Inflammation, atrophy, and gastric cancer. *J Clin Invest* 2007; **117**: 60–69.
4 Coussens LM, Werb Z. Inflammation and cancer. *Nature* 2002; **420**: 860–867.
5 Grivennikov SI, Greten FR, Karin M. Immunity, inflammation, and cancer. *Cell* 2010; **140**: 883–899.
6 El-Omar EM, Carrington M, Chow W-H, McColl KE, Bream JH, Young HA *et al.* Interleukin-1 polymorphisms associated with increased risk of gastric cancer. *Nature* 2000; **404**: 398–402.
7 EL-Omar EM, Rabkin CS, Gammon MD, Vaughan TL, Risch HA, Schoenberg JB *et al.* Increased risk of noncardia gastric cancer associated with proinflammatory cytokine gene polymorphisms. *Gastroenterology* 2003; **124**: 1193–1201.
8 Mochado JC, Figueiredo C, Canedo P, Pharoah P, Carvalho R, Nabais S *et al.* A proinflammatory genetic profile increases the risk for chronic atrophic gastritis and gastric carcinoma. *Gastroenterology* 2003; **125**: 364–371.
9 El-Omar EM. Role of host genes in sporadic gastric cancer. *Best Pract Res Clin Gastroenterology* 2006; **20**: 675–686.
10 Tu S, Bhagat G, Cui G, Takaishi S, Kurt-Jones EA *et al.* Overexpression of interleukin-1β induces gastric inflammation and cancer mobilizes myeloid-derived suppressor cells in mice. *Cancer Cell* 2008; **14**: 408–419.
11 Tebbutt NC, Giraud AS, Inglese M, Jenkins B, Waring P, Clay FJ *et al.* Reciprocal regulation of gastrointestinal homeostasis by SHP2 and STAT-mediated trefoil gene activation in gp130 mutant mice. *Nat Med* 2002; **8**: 1089–1097.
12 Tye H, Kennedy CL, Najdovska M, McLeod L, McCormack W, Hughes N *et al.* STAT3-driven upregulation of TLR2 promotes gastric tumorigenesis independent of tumor inflammation. *Cancer Cell* 2012; **22**: 466–478.
13 Balkwill F. TNF-α in promotion and progression of cancer. *Cancer Metastasis Rev* 2006; **25**: 409–416.
14 Balkwill F. Tumor necrosis factor and cancer. *Nat Rev Cancer* 2009; **9**: 361–371.
15 Moore RJ, Owens DM, Stamp G, Arnott C, Burke F, East N *et al.* Mice deficient in tumor necrosis factor-α are resistant to skin carcinogenesis. *Nat Med* 1999; **5**: 828–831.
16 Arnott CH, Scott KA, Moore RJ, Robinson SC, Thompson RG, Balkwill FR. Expression of both TNF-α receptor subtypes is essential for optimal skin tumour development. *Oncogene* 2004; **23**: 1902–1910.
17 Popivanova BK, Kitamura K, Wu Y, Kondo T, Kagaya T, Kanoko S *et al.* Blocking TNF-α in mice reduces colorectal carcinogenesis associated with chronic colitis. *J Clin Invest* 2008; **118**: 560–570.
18 Oshima H, Matsunaga A, Fujimura T, Tsukamoto T, Taketo MM, Oshima M. Carcinogenesis in mouse stomach by simultaneous activation of the Wnt signaling and prostaglandin E_2 pathway. *Gastroenterology* 2006; **131**: 1086–1095.
19 Oshima H, Oguma K, Du YC, Oshima M. Prostaglandin E_2, Wnt and BMP in gastric tumor mouse models. *Cancer Sci* 2009; **100**: 1779–1785.
20 Clements WM, Wang J, Sarnaik A, Kim OJ, MacDonald J, Fenoglio-Preiser C *et al.* *β-Catenin* mutation is a frequent cause of Wnt pathway activation in gastric cancer. *Cancer Res* 2002; **62**: 3503–3506.
21 Wang D, DuBois RN. Eicosanoids and cancer. *Nat Rev Cancer* 2010; **10**: 181–193.
22 Itadani H, Oshima H, Oshima M, Kotani H. Mouse gastric tumor models with prostaglandin E_2 pathway activation show similar gene expression profiles to intestinal-type human gastric cancer. *BMC Genomics* 2009; **10**: 615.
23 Oshima H, Hioki K, Popivanova BK, Oguma K, van Rooijen N, Ishikawa TO *et al.* Prostaglandin E_2 signaling and bacterial infection recruit tumor-promoting macrophages to mouse gastric tumors. *Gastroenterology* 2011; **140**: 596–607.
24 Itzkovitz S, Lyubimova A, Blat IC, Maynard M, van Es J, Lees J *et al.* Single-molecule transcript counting of stem-cell markers in the mouse intestine. *Nat Cell Biol* 2012; **14**: 106–114.
25 Huch M, Dorrell C, Boj SF, van Es JH, Li VS, van de Watering M *et al.* *In vitro* expansion of single $Lgr5^+$ liver stem cells induced by Wnt-driven regeneration. *Nature* 2013; **494**: 247–250.
26 Ishimoto T, Oshima H, Oshima M, Kai K, Torii R, Masuko T *et al.* $CD44^+$ slow-cycling tumor cell expansion is triggered by cooperative actions of Wnt and prostaglandin E_2 in gastric tumorigenesis. *Cancer Sci* 2010; **101**: 673–678.
27 Ishimoto T, Nagano O, Yae T, Tamada M, Motohara T, Oshima H *et al.* CD44 variant regulates redox status in cancer cells by stabilizing the xCT subunit of system xc(-) and thereby promotes tumor growth. *Cancer Cell* 2011; **19**: 387–400.
28 Zöller M. CD44: can a cancer-initiating cell profit from an abundantly expressed molecule? *Nat Rev Cancer* 2011; **11**: 254–267.
29 Barker N, Huch M, Kujala P, van de Wetering M, Snippert HJ, van Es JH *et al.* $Lgr5^{+ve}$ stem cells drive self-renewal in the stomach and build long-lived gastric units in vitro. *Cell Stem Cell* 2011; **6**: 25–36.
30 Kulbe H, Chakravarty P, Leinster DA, Charles KA, Kwong J, Thompson RG *et al.* A dynamic inflammatory cytokine network in the human ovarian cancer microenvironment. *Cancer Res* 2012; **71**: 66–75.
31 Seno H, Oshima M, Ishikawa TO, Oshima H, Takaku K, Chiba T *et al.* Cyclooxygenase 2-and prostaglandin E_2 receptor EP_2-dependent angiogenesis in $Apc^{\Delta 716}$ mouse intestinal polyps. *Cancer Res* 2002; **62**: 506–511.
32 Castellone MD, Teramoto H, Williams BO, Druey KM, Gutkind JS. Prostaglandin E_2 promotes colon cancer cell growth through a Gs-axin-β-catenin signaling axis. *Science* 2005; **310**: 1504–1510.
33 Oguma K, Oshima H, Aoki M, Uchio R, Naka K, Nakamura S *et al.* Activated macrophages promote Wnt signalling through tumour necrosis factor-αin gastric tumour cells. *EMBO J* 2008; **27**: 1671–1681.
34 Bollrath J, Phesse TJ, von Burstin VA, Putoczki T, Bennecke M, Bateman T *et al.* gp130-mediated Stat3 activation in enterocytes regulates cell survival and cell-cycle progression during colitis-associated tumorigenesis. *Cancer Cell* 2009; **15**: 91–102.
35 Grivennikov S, Karin E, Terzic J, Mucida D, Yu G-Y, Vallabhapurapu S *et al.* IL-6 and Stat3 are required for survival of intestinal epithelial cells and development of colitis-associated cancer. *Cancer Cell* 2009; **15**: 103–113.
36 Acharyya S, Oskarsson T, Vanharanta S, Malladi S, Kim J, Morris PG *et al.* A CXCL1 paracrine network links cancer chemoresistance and metastasis. *Cell* 2012; **150**: 165–178.
37 Block D, Gorin Y. Aiding and abetting roles of NOX oxidases in cellular transformation. *Nat Rev Cancer* 2012; **12**: 627–637.
38 Mitsushita J, Lambeth JD, Kamata T. The superoxide-generating oxidase Nox1 is functionally required for Ras oncogene transformation. *Cancer Res* 2004; **64**: 3580–3585.
39 Adachi Y, Shibai Y, Mitsushita J, Shang WH, Hirose K, Kamata T. Oncogenic Ras upregulates NADPH oxidase 1 gene expression through MEK-ERK-dependent phosphorylation of GATA-6. *Oncogene* 2008; **27**: 4921–4932.

© 2013 Macmillan Publishers Limited

40 Juhasz A, Ge Y, Markel S, Chiu A, Matsumoto L, van Balgooy J *et al.* Expression of NADPH oxidase homologues and accessory genes in human cancer cell lines, tumours and adjacent normal tissues. *Free Radic Res* 2009; **43**: 523–532.
41 Kostenis E, Waelbroeck M, Milligan G. Techniques: Promiscous Gα proteins in basic research and drug discovery. *TrendsPham Sci* 2005; **26**: 595–602.
42 Liu AMF, Wong YH. Activation of nuclear factor κB by somatostatin type 2 receptor in pancreatic acinar AR42J cells involves $G\alpha_{14}$ and multiple signaling components. *J Biol Chem* 2005; **280**: 34617–34625.
43 Lee MMK, Wong YH. CCR1-mediated activation of nuclear factor-κB in THP-1 monocytic cells involves *pertussis* toxin-insensitive $G\alpha_{14}$ and $G\alpha_{16}$ signaling cascade. *J Leukoc Biol* 2009; **86**: 1319–1329.
44 Schwitalla S, Fingerle AA, Cammareri P, Nebelsiek T, Göktuna SI, Ziegler PK *et al.* Intestinal tumorigenesis initiated by dedifferentiation and acquisition of stem-cell-like properties. *Cell* 2013; **152**: 25–38.
45 Kong D, Piao Y-S, Yamashita S, Oshima H, Oguma K, Fushida S *et al.* Inflammation-induced repression of tumor suppressor miR-7 in gastric tumor cells. *Oncogene* 2012; **31**: 3949–3960.

This work is licensed under a Creative Commons Attribution-NonCommercial-ShareAlike 3.0 Unported License. To view a copy of this license, visit http://creativecommons.org/licenses/by-nc-sa/3.0/

Supplementary Information accompanies this paper on the Oncogene website (http://www.nature.com/onc)

© 2013 Macmillan Publishers Limited

Biochemical Pharmacology xxx (2014) xxx–xxx

Contents lists available at ScienceDirect

Biochemical Pharmacology

journal homepage: www.elsevier.com/locate/biochempharm

DIF-1 inhibits tumor growth *in vivo* reducing phosphorylation of GSK-3β and expressions of cyclin D1 and TCF7L2 in cancer model mice

Fumi Takahashi-Yanaga [a,b,*], Tatsuya Yoshihara [a], Kentaro Jingushi [a], Kazuhiro Igawa [c], Katsuhiko Tomooka [c], Yutaka Watanabe [d], Sachio Morimoto [a], Yoshimichi Nakatsu [e], Teruhisa Tsuzuki [e], Yusaku Nakabeppu [f], Toshiyuki Sasaguri [a,*]

[a] Department of Clinical Pharmacology, Faculty of Medical Sciences, Kyushu University, Fukuoka, Japan
[b] Global Medical Science Education Unit, Faculty of Medical Sciences, Kyushu University, 3-1-1 Maidashi, Higashi-ku, Fukuoka 812-8582, Japan
[c] Department of Molecular and Material Science, Institute for Materials Chemistry and Engineering, Kyushu University, Fukuoka, Japan
[d] Department of Applied Chemistry, Faculty of Engineering, Ehime University, Matsuyama, Japan
[e] Department of Medical Biophysics and Radiation Biology, Faculty of Medical Sciences, Kyushu University, Fukuoka, Japan
[f] Division of Neurofunctional Genomics, Department of Immunobiology and Neuroscience, Medical Institute of Bioregulation, Kyushu University, Fukuoka, Japan

ARTICLE INFO

Article history:
Received 10 February 2014
Received in revised form 12 March 2014
Accepted 14 March 2014
Available online xxx

Keywords:
DIF-1
TCF7L2
GSK-3β
Wnt/β-catenin signaling pathway
Egr-1

ABSTRACT

We reported that differentiation-inducing factor-1 (DIF-1), synthesized by *Dictyostelium discoideum*, inhibited proliferation of various tumor cell lines *in vitro* by suppressing the Wnt/β-catenin signaling pathway. However, it remained unexplored whether DIF-1 also inhibits tumor growth *in vivo*. In the present study, therefore, we examined *in-vivo* effects of DIF-1 using three cancer models: *Mutyh*-deficient mice with oxidative stress-induced intestinal tumors and nude mice xenografted with the human colon cancer cell line HCT-116 and cervical cancer cell line HeLa. In exploration for an appropriate route of administration, we found that orally administered DIF-1 was absorbed through the digestive tract to elevate its blood concentration to levels enough to suppress tumor cell proliferation. Repeated oral administration of DIF-1 markedly reduced the number and size of intestinal tumors that developed in *Mutyh*-deficient mice, reducing the phosphorylation level of GSK-3β Ser^9 and the expression levels of early growth response-1 (Egr-1), transcription factor 7-like 2 (TCF7L2) and cyclin D1. DIF-1 also inhibited the growth of HCT-116- and HeLa-xenograft tumors together with decreasing phosphorylation level of GSK-3β Ser^9, although it was not statistically significant in HeLa-xenograft tumors. DIF-1 also suppressed the expressions of Egr-1, TCF7L2 and cyclin D1 in HCT-116-xenograft tumors and those of β-catenin, TCF7L2 and cyclin D1 in HeLa-xenograft tumors. This is the first report to show that DIF-1 inhibits tumor growth *in vivo*, consistent with its *in-vitro* action, suggesting that this compound may have potential as a novel anti-tumor agent.

© 2014 Elsevier Inc. All rights reserved.

1. Introduction

The Wnt/β-catenin signaling pathway, which is well conserved throughout biological evolution, regulates a number of cellular functions during embryonic development and in maintenance of tissue homeostasis by regulating somatic stem cells and their niches [1–3]. Accumulating evidence suggests that this pathway is often involved in oncogenesis and cancer development. Activation of the Wnt/β-catenin signaling pathway results in upregulation of its target genes, such as *CCND1* encoding cyclin D1 and *c-myc*, which play key roles in the initiation and progression of G_1 phase in the cell cycle [4,5], thereby promoting tumor formation [6–9]. In fact, this pathway is constitutively activated in most colorectal cancers, including those in patients with familial adenomatous polyposis (FAP), and other types of malignant tumors [10–14].

Glycogen synthase kinase-3β (GSK-3β) was first identified as a cytoplasmic serine/threonine protein kinase that phosphorylates glycogen synthase to inhibit its activity. However, it is now well known that this kinase plays central roles in various biological

* Corresponding authors at: Department of Clinical Pharmacology, Faculty of Medical Sciences, Kyushu University, 3-1-1 Maidashi, Higashi-ku, Fukuoka 812-8582, Japan. Tel.: +81 92 642 6887; fax: +81 92 642 6084.
E-mail addresses: yanaga@cliphrarm.med.kyushu-u.ac.jp (F. Takahashi-Yanaga), sasaguri@cliphrarm.med.kyushu-u.ac.jp (T. Sasaguri).

http://dx.doi.org/10.1016/j.bcp.2014.03.006
0006-2952/© 2014 Elsevier Inc. All rights reserved.

processes including the Wnt/β-catenin signaling pathway [15,16]. GSK-3β inhibits the Wnt/β-catenin signaling pathway by phosphorylating β-catenin to accelerate its proteolysis [15,17], resulting in the inhibition of transcription of *CCND1*, *c-myc* and other Wnt target genes. In addition, GSK-3β phosphorylates cyclin D1 to promote its degradation. Accordingly, GSK-3β reduces cyclin D1 expression by two mechanisms: inhibition of *CCND1* gene transcription and promotion of cyclin D1 protein degradation [17,18]. Therefore, we thought the compounds that induce GSK-3β activation could be useful as anti-tumor agents.

We previously reported that differentiation-inducing factors (DIF-1 and DIF-3), which were identified in *Dictyostelium discoideum* as putative morphogens required for stalk cell differentiation [19,20], have a powerful antiproliferative effect on human cancer cell lines *in vitro* [21–27]. With regard to the underlying mechanisms, we revealed that DIFs accelerated degradation of cyclin D1 and β-catenin through the activation of GSK-3β, leading to the suppression of the Wnt/β-catenin signaling pathway and cell cycle arrest at the G_0/G_1 phase in various human cells [21–26]. Surprisingly, DIF-1 also suppressed proliferation of colon cancer cells in which the Wnt/β-catenin signaling pathway was constitutively activated by lack of β-catenin destruction mechanisms. In this regard, we revealed that DIF-1 suppressed transcription factor 7-like 2 (TCF7L2) expression via reduced early growth response-1 (Egr-1) protein amount, thereby inhibiting the Wnt/β-catenin signaling pathway without affecting β-catenin expression level [27]. However, the mechanisms for DIF-1's *in-vivo* action remain to be clarified.

Therefore, in the present study, to assess whether DIF-1 is applicable to the treatment of malignant tumors, we examined its *in-vivo* effects using mice. First, we examined its pharmacokinetics and toxicity. Second, we evaluated the anti-cancer effects of DIF-1 using a spontaneous cancer model and human cancer xenograft models. For the former, we employed *Mutyh*-deficient (*Mutyh*$^{-/-}$) mice, which lack the MutY homolog (MUTYH), a mammalian DNA glycosylase that initiates base excision repair, and is thus susceptible to oxidative stress-induced carcinogenesis [28–31]. These mice provide a useful animal model for examining colorectal adenoma and carcinoma [31]. For the latter, we used nude mice bearing HCT-116 cells and those bearing HeLa cells. Using these cancer models, we show for the first time that orally administered DIF-1 exhibits anti-tumor effects *in vivo*. Third, we examined the mechanisms for DIF-1's *in-vivo* actions.

2. Materials and methods

2.1. Chemicals and antibodies

DIF-1 (1-(3,5-dichloro-2, 6-dihydroxy-4-methoxyphenyl)-1-hexanone) was synthesized as described previously (purity: >98%) [32]. Celecoxib was kindly provided by Pfizer (New York, NY, USA). An anti-cyclin D1 polyclonal antibody was purchased from Santa Cruz Biotechnology (Santa Cruz, CA, USA). Anti-β-catenin and anti-GSK-3β monoclonal antibodies were purchased from R&D Systems (Minneapolis, MN, USA). Anti-Egr-1 monoclonal antibody, anti-transcription factor 7-like 2 (TCF7L2) monoclonal antibody (6H5-3) and anti-phospho-GSK-3β (Ser^9) polyclonal antibody were purchased from Cell Signaling Technology (Danvers, MA, USA). An anti-GAPDH monoclonal antibody was purchased from Abcam (Cambridge, MA, USA). An anti-α-tubulin monoclonal antibody was purchased from Calbiochem (Darmstadt, Germany). Growth factor-reduced Matrigel was obtained from BD Biosciences (San Jose, CA, USA).

2.2. Cell culture

HCT-116 and HeLa cells were grown in Dulbecco's modified Eagle's medium (Sigma, St. Louis, MO, USA) supplemented with 10% fetal bovine serum, 100 U/mL penicillin G, and 0.1 μg/mL streptomycin.

2.3. Western blot analysis

Protein samples (10 μg/lane) were separated by 12% SDS–polyacrylamide gel electrophoresis and then transferred to a polyvinylidene difluoride membrane using a semi-dry transfer system (1 h at 12 V). Western blot analysis was performed as described previously [21]. Optical densitometric scans were performed using NIH Image J software.

2.4. Administration of DIF-1

For intraperitoneal administration, 30 mg/kg DIF-1, pounded in a mortar and suspended in PBS, was injected into the abdomens of C57BL/6J male mice (10–11 weeks old; Kyudo, Tosu, Japan). For oral administration, DIF-1 was suspended in a 0.25% methylcellulose solution or dissolved in soybean oil. These DIF-1-containing solutions were then orally administered to the C57BL/6J mice.

2.5. Measurement of the DIF-1 concentration in mouse plasma

Mouse blood samples were collected by cardiac puncture at the indicated times, and plasma was isolated by centrifugation at 500 × *g* for 15 min. The plasma concentration of DIF-1 was determined by a reverse phase high-performance liquid chromatography (HPLC) system (Waters 2695, Milford, MA, USA) as described previously [33] with a slight modification. Briefly, mouse plasma samples (200 μL) containing 500 ng daisein (Wako Pure Chemical Industries Ltd., Osaka, Japan) as an internal standard were mixed with 200 μL chloroform. After mixing, the solution was centrifuged at 13,000 × *g* for 5 min, and then the organic phase was separated and evaporated. The residue was dissolved in 80 μL of a mixture of acetic acid (5%, v/v) and methanol (40%, v/v). A sample (50 μL) was then applied to a column for separation (TSKgel ODS-80Ts; Tosoh Corporation, Tokyo, Japan). The samples were eluted by a linear gradient of methanol (40–95%) in the presence of 5% acetic acid over 40 min at a flow rate of 1.0 mL/min. A UV detector was operated at 277 nm. A calibration curve was prepared by plotting the area ratios of DIF-1 normalized to the internal standard.

2.6. Intestinal tumor model mice

Intestinal tumors (adenomas and carcinomas) were formed by methods reported previously with slight modifications [31]. Briefly, $KBrO_3$ dissolved in drinking water at a concentration of 2 g/L was provided to 4-week-old mice for 12 weeks. At 16 weeks of age, the mice were randomly divided into six groups (six mice including three males and three females in each group). Mice in test groups were orally administered with DIF-1 or celecoxib, which was suspended in a 0.25% methylcellulose solution, once a day for 5 days/week over 4 weeks. Control mice received the vehicle only. The body weight of the mice was monitored weekly. At 20 weeks of age, all mice were sacrificed to obtain blood and intestinal samples. Blood samples were analyzed by a Celltac-alpha MEK-6358 (Nihon Kohden, Tokyo, Japan) for blood cell counts. Intestines were fixed in 4% formaldehyde, and the tumors were observed under a microscope. Images of the tumors were obtained and analyzed using NIH Image J software. For Western blot analysis, intestinal tissues (2 cm down from the pylorus) were homogenized in Laemmli's sample buffer immediately after

Please cite this article in press as: Takahashi-Yanaga F, et al. DIF-1 inhibits tumor growth *in vivo* reducing phosphorylation of GSK-3β and expressions of cyclin D1 and TCF7L2 in cancer model mice. Biochem Pharmacol (2014), http://dx.doi.org/10.1016/j.bcp.2014.03.006

resection. After adjustment of the protein content, the samples were electrophoresed and blotted with antibodies. Intestinal bleeding was examined in excrement by the guaiac reaction (Sionogi II test; Sionogi, Osaka, Japan).

2.7. Human cancer xenograft model mice

Eight-week-old female mice (BALB/c nu/nu) were subcutaneously injected in their right flank with 400 μL Matrigel and 5×10^6 human cancer cells (HCT-116 or HeLa) suspended in PBS (1:1, v:v). Mice were randomly divided into DIF-1 treatment and control groups. At the beginning, DIF-1 was suspended in a 0.25% methylcellulose solution and orally administered as in the experiment with intestinal tumor model mice. However, later, we improved the administration method to elevate plasma concentrations of DIF-1 by dissolving DIF-1 in soybean oil and dosing every 12 h (300 mg/kg in the morning and 150 mg/kg in the evening) for 5 days/week. Control group mice received the vehicles only. The body weight of mice was monitored weekly. Tumors removed on the indicated days were measured for size and weight, and then prepared for Western blot analysis. Blood samples were collected and analyzed for blood cell counts.

2.8. Statistical analysis

Results are expressed as the means ± s.e.m. Statistical analyses of differences between two mean values were performed using the Student's *t*-test. Multiple mean values were compared by one-way ANOVA with the Dunnett's multiple comparison test.

2.9. Ethics information

The study protocol was approved by the Committee of Ethics on Animal Experiments at Kyushu University (Permit Number: A22-046-0). Animal handling and procedures were carried out in compliance with the Guidelines for Animal Experiments, Kyushu University, and the Law (No. 105) and Notification (No. 6) of the Japanese Government. All surgeries were performed under sodium pentobarbital anesthesia, and all efforts were made to minimize suffering.

3. Results

3.1. Plasma concentration of DIF-1 in mice

To examine whether plasma DIF-1 concentrations reach levels that can show an antiproliferative effect on tumor cells, we measured DIF-1 concentrations after intraperitoneal and oral administration in wild-type C57BL/6J mice using a HPLC system. After intraperitoneal injection, the DIF-1 concentration rapidly increased and reached maximal levels (20–30 μg/mL) within 30 min, followed by a rapid decline (Fig. 1A). When orally administered, the DIF-1 concentration reached maximal levels (30–40 μg/mL) within 1 h, and the decline was much slower compared with that following intraperitoneal injection (Fig. 1B). Because the EC_{50} value of DIF-1 for an *in vitro* antiproliferative effect is 5–8 μg/mL, these results suggest that the plasma concentration of DIF-1 can be sufficiently elevated to show an

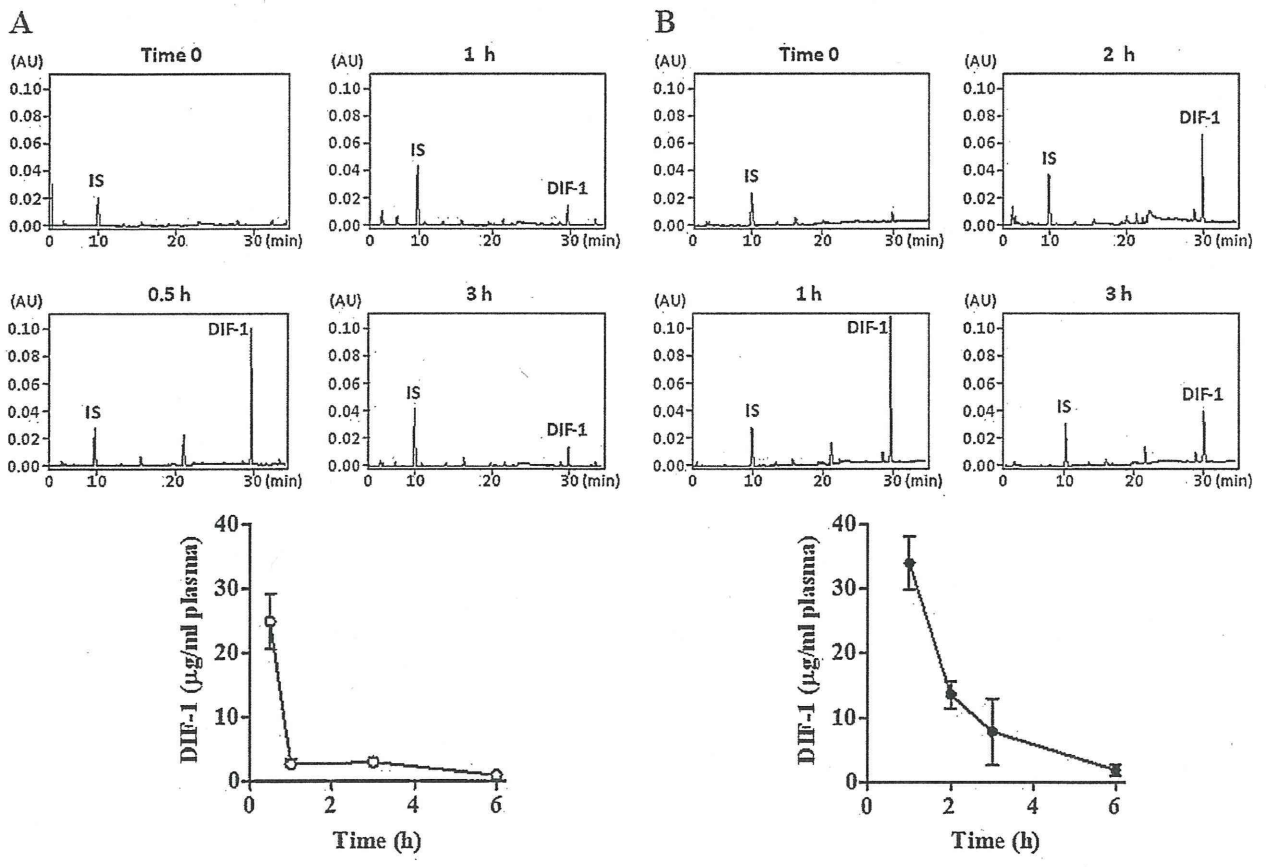

Fig. 1. Plasma concentrations of DIF-1.
DIF-1 was administered to mice intraperitoneally (A) or orally (B). Blood was collected at the indicated times to prepare HPLC samples. Upper panels: HPLC elution profiles. Lower panels: time course of plasma DIF-1 concentrations. Values are the means ± s.e.m. ($n = 3$). IS, internal standard.

Please cite this article in press as: Takahashi-Yanaga F, et al. DIF-1 inhibits tumor growth *in vivo* reducing phosphorylation of GSK-3β and expressions of cyclin D1 and TCF7L2 in cancer model mice. Biochem Pharmacol (2014), http://dx.doi.org/10.1016/j.bcp.2014.03.006

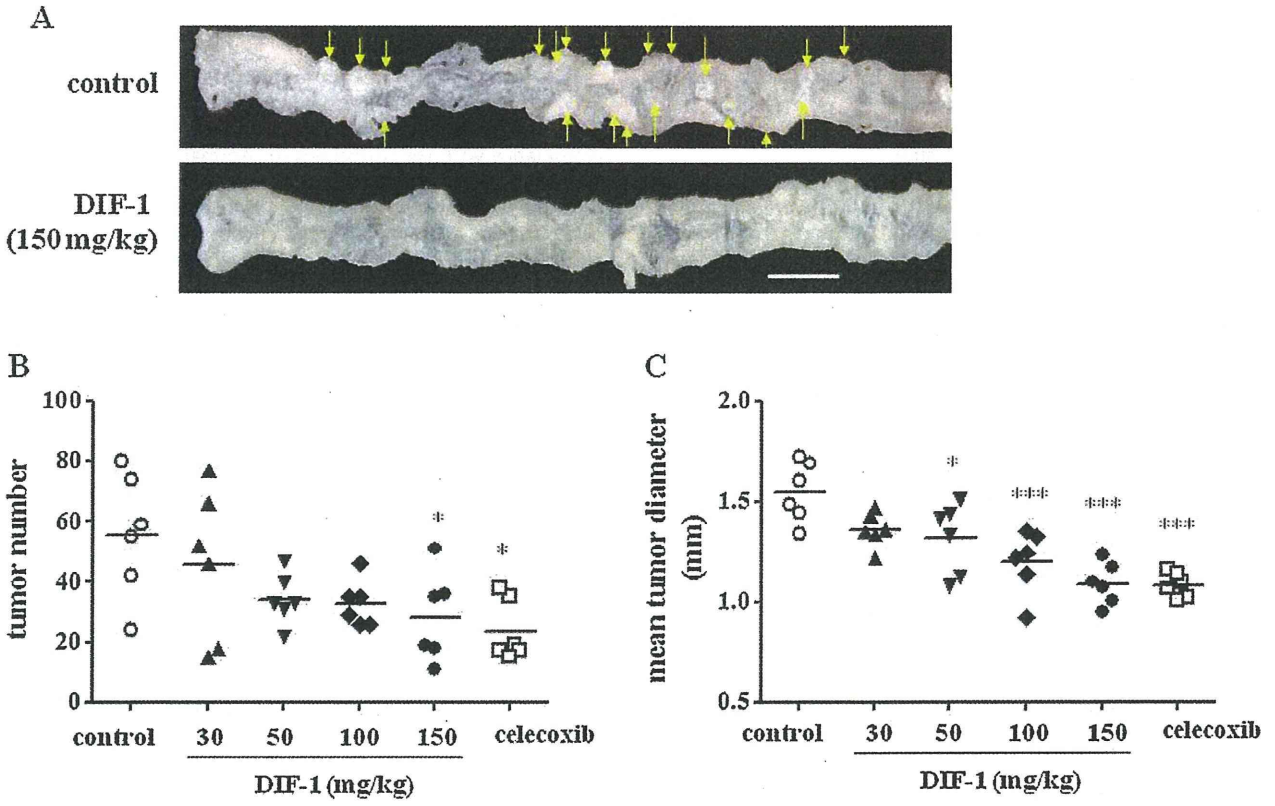

Fig. 2. Effect of DIF-1 on intestinal tumors induced by $KBrO_3$ in *Mutyh*$^{-/-}$ mice.
A. Proximal region of the small intestines. Scale bar indicates 1 cm. Arrows indicate tumors with a >2.5 mm diameter. B. Tumor numbers are plotted for each mouse. Horizontal bars indicate the means of each group ($n = 6$). C. Mean tumor diameters are plotted for each mouse. Horizontal bars indicate the means of each group ($n = 6$). $^{*}P < 0.05$ vs. control, $^{***}P < 0.001$ (one-way ANOVA with Dunnett's multiple comparison test).

antiproliferative effect *in vivo*. Therefore, we used oral administration for the following experiments.

3.2. Effect of DIF-1 on oxidative stress-induced tumors in *Mutyh*$^{-/-}$ mice

To evaluate the anti-tumor effect of DIF-1 *in vivo*, we first used mice deficient for MUTYH, an enzyme that prevents formation of oxidative stress-induced DNA lesions. Studies have shown that MUTYH deficiency might be involved in the development of colorectal adenoma and carcinoma in humans [28–30]. As we reported previously [31], the occurrence of carcinomas in the small intestine was dramatically increased by oxidative stress in *Mutyh*$^{-/-}$ mice. Twelve weeks of treatment with 0.2% $KBrO_3$, a strong oxidant, followed by vehicle treatment for 4 weeks induced numerous intestinal tumors (55.7 ± 8.4, $n = 6$) in *Mutyh*$^{-/-}$ mice, whereas only a small number of tumors were formed in wild-type mice (1.2 ± 0.5, $n = 6$).

We administered DIF-1 or celecoxib to *Mutyh*$^{-/-}$ mice for 4 weeks to examine the effects of these compounds. We used celecoxib for reference because it has been used for the treatment of FAP patients [34]. DIF-1 treatment (10–150 mg/kg/day for 4 weeks) markedly reduced the number and size of intestinal tumors in a dose-dependent manner (Fig. 2A–C). The effectiveness of DIF-1 appeared to be comparable with that of celecoxib, because the same doses (150 mg/kg) of these compounds showed similar effects.

Next, we carried out Western blot analyses of tumor samples obtained from vehicle- or DIF-1 (150 mg/kg)-treated mice. Because DIF-1 activates GSK-3β by dephosphorylation of Ser^9 in cultured cells [22,23,25], we analyzed the effect of DIF-1 on the phosphorylation status of GSK-3β Ser^9 in the intestines. As shown in Fig. 3A, DIF-1 significantly decreased the phosphorylation level of GSK-3β Ser^9, suggesting that DIF-1 also activated GSK-3β *in vivo*. Furthermore, DIF-1 markedly decreased the protein expression levels of Egr-1, TCF7L2 and cyclin D1, although β-catenin levels were unaltered (Fig. 3B). These results suggested that DIF-1 inhibited tumor growth in *Mutyh*$^{-/-}$ mice by GSK-3β-mediated suppression of cyclin D1 expression and Egr-1-mediated suppression of TCF7L2 expression.

To examine whether long-term treatment with DIF-1 shows adverse effect on the general condition, we measured their body weight and peripheral blood cell counts, as well as observing their appearance and activity. Red blood cell (RBC) numbers and hemoglobin (Hb) concentrations were significantly lower in *Mutyh*$^{-/-}$ mice compared with those in wild-type mice (Table 1). *Mutyh*$^{-/-}$ mice may have suffered from anemia caused by intestinal bleeding due to developed tumors, because excrement from *Mutyh*$^{-/-}$ mice was strongly positive (+++) for occult blood, whereas excrement from wild-type mice was negative (data not shown). There were no significant differences in white blood cell (WBC) or platelet numbers and changes in body weight (ΔBW) between *Mutyh*$^{-/-}$ mice and wild-type mice. Administration of DIF-1 or celecoxib did not affect the appearance, activity, WBC and platelet numbers, or ΔBW of the mice. However, DIF-1 and celecoxib significantly increased RBC counts and Hb levels, suggesting that these compounds prevent bleeding from the intestinal mucosa by reducing size and number of tumors (Table 1).

Please cite this article in press as: Takahashi-Yanaga F, et al. DIF-1 inhibits tumor growth *in vivo* reducing phosphorylation of GSK-3β and expressions of cyclin D1 and TCF7L2 in cancer model mice. Biochem Pharmacol (2014), http://dx.doi.org/10.1016/j.bcp.2014.03.006

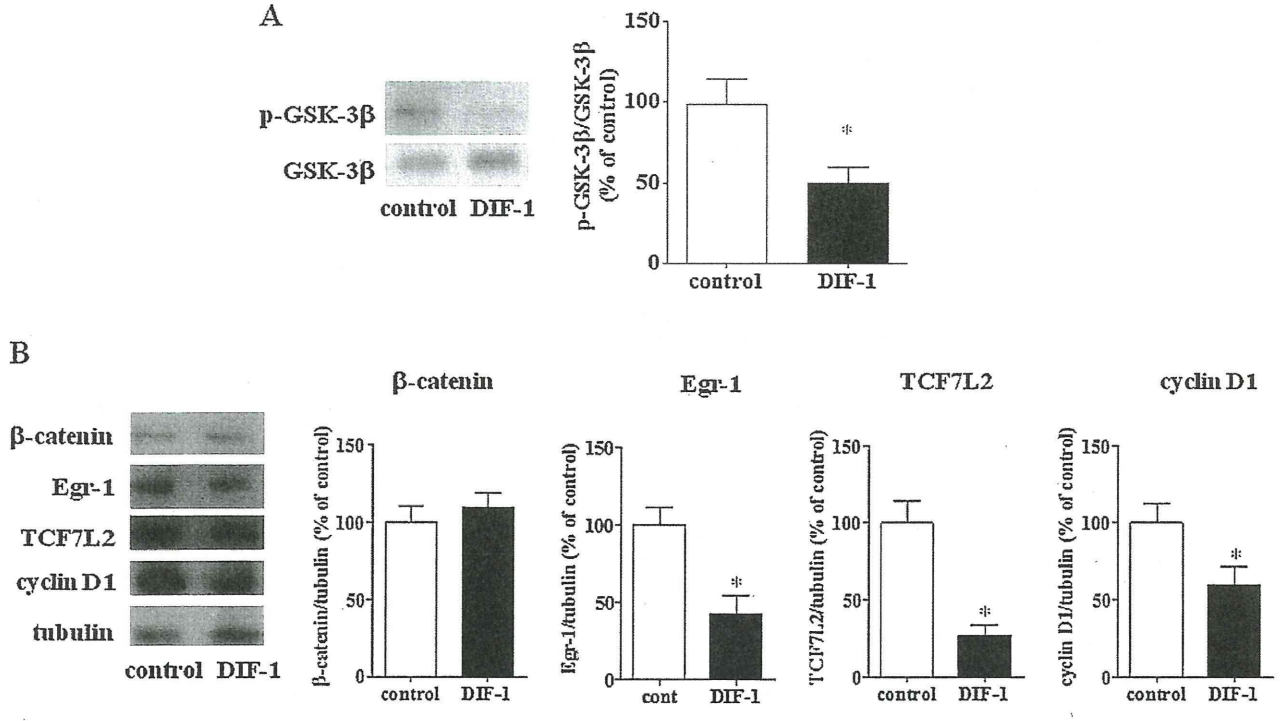

Fig. 3. Western blot analyses of proteins extracted from *Mutyh*$^{-/-}$ mouse small intestines.
Protein samples prepared from the small intestines of vehicle- and DIF-1 (150 mg/kg)-treated mice were analyzed by Western blotting. A. GSK-3β phosphorylation levels. Protein samples were subjected to Western blotting to analyze phosphorylation of GSK-3β Ser^{9} using an anti-phospho-GSK-3β antibody. After stripping, the membranes were reprobed with an anti-GSK-3β antibody. Band densities are shown as percentages of the controls. Values are the means ± s.e.m. (n = 6). *P < 0.05 vs. control (Student's t-test). p-GSK-3β, phospho-GSK-3β. B. Expression levels of β-catenin, Egr-1, TCF7L2, and cyclin D1. Band densities were quantified and normalized to those of tubulin. Values are the means ± s.e.m. (n = 6). *P < 0.05 vs. control (Student's t-test).

3.3. Effect of DIF-1 on human cancer xenografts

Our experiments using *Mutyh*$^{-/-}$ mice showed that DIF-1 inhibited intestinal tumor growth. However, it appeared possible that DIF-1 administered into the digestive tract directly acted on the intestinal mucosa without absorption into systemic circulation. Therefore, we investigated whether orally administered DIF-1 could show an anti-tumor effect on tumors growing in a region distant from the digestive tract. For this purpose, we employed nude mice xenografted with two different cell species of human cancer: HCT-116-xenografted mice to examine the effect of DIF-1 on colon cancer *in vivo* and HeLa-xenografted mice to confirm the effect of DIF-1 in a different cancer. One reason that we chose these two cancer cell species was that the β-catenin destruction mechanism is mutated in HCT-116 but it is intact in HeLa cells. We first treated these xenografted mice with orally administered DIF-1 (150 mg/kg every 24 h) that was suspended in 0.25% methylcellulose (the same solvent used in Mutyh$^{-/-}$ mice experiments). However, DIF-1 failed to show a significant effect on tumor xenografts (data not shown). We considered that this

Table 1
Effects of DIF-1 on blood cell counts and body weight.

		WBC (×10^2 cells/μL)	RBC (×10^4 cells/μL)	Hb (g/dL)	Plt (×10^4 cells/μL)	ΔBW (g)
Wild-type						
Vehicle		58.0 ± 5.7	923.3 ± 16.3	12.2 ± 0.38	52.7 ± 5.5	3.26 ± 0.77
Mutyh$^{-/-}$						
Vehicle		54.6 ± 6.1	615.7 ± 66.4**	10.0 ± 0.93*	64.7 ± 9.5	1.75 ± 0.36
DIF-1	mg/kg					
	10	50.5 ± 6.6	678.8 ± 60.0**	10.6 ± 0.38	65.0 ± 7.9	1.85 ± 0.53
	30	43.7 ± 7.2	682.3 ± 67.0**	11.0 ± 0.69	74.3 ± 5.3	1.87 ± 0.36
	100	65.2 ± 13.1	752.0 ± 34.7	11.6 ± 0.40	58.4 ± 3.9	1.93 ± 0.50
	150	55.9 ± 4.1	787.3 ± 37.7	11.7 ± 0.41	73.0 ± 7.0	2.16 ± 0.66
Celecoxib	mg/kg					
	150	53.5 ± 12.7	828.3 ± 29.1	11.6 ± 0.38	64.1 ± 6.6	2.51 ± 0.53

DIF-1, celecoxib or the vehicle (methylcellulose) was orally administered to mice for 4 weeks. Data represent the means ± s.e.m. Statistical significance was determined by one-way ANOVA with Dunnett's multiple comparison test. N = 6 for each group. WBCs, white blood cells; RBCs, red blood cells; Hb, hemoglobin; Plt, platelets; ΔBW, body weight change from 12 to 16 weeks.
* P < 0.05 vs. vehicle-treated wild-type mice.
** P < 0.01 vs. vehicle-treated wild-type mice.

Please cite this article in press as: Takahashi-Yanaga F, et al. DIF-1 inhibits tumor growth *in vivo* reducing phosphorylation of GSK-3β and expressions of cyclin D1 and TCF7L2 in cancer model mice. Biochem Pharmacol (2014), http://dx.doi.org/10.1016/j.bcp.2014.03.006

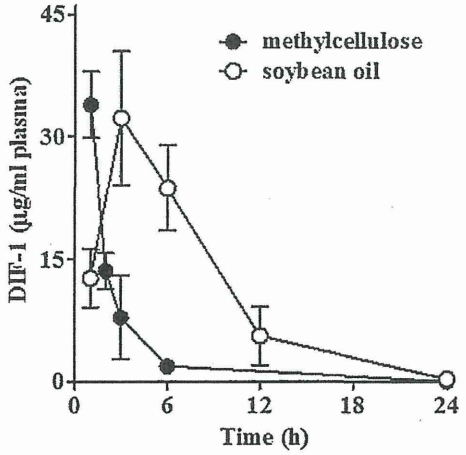

Fig. 4. Improvement of DIF-1 pharmacokinetics by dissolving it in soybean oil. Mice orally received DIF-1 suspended in methylcellulose or dissolved in soybean oil. Blood was collected at indicated times after administration and measured for plasma DIF-1 concentration using an HPLC system. $N = 3$ for each time point. Methylcellulose data (1–6 h) are the same as those shown in Fig. 1B.

observation might result from the difficulty to maintain a sufficient concentration of DIF-1 for more than 3 h (Fig. 1B).

After exploration of a method to increase DIF-1 plasma concentration, we found that soybean oil was a better solvent than methylcellulose. This effect was probably observed because of enhanced absorption, although the trough concentration at 24 h was still very low (Fig. 4). Therefore, we treated tumor-bearing nude mice with DIF-1 dissolved in soybean oil every 12 h (300 mg/kg in the morning and 150 mg/kg in the evening for 5 days/week).

As shown in Fig. 5A, DIF-1 administered in this manner significantly suppressed the growth of HCT-116-xenograft tumor masses and the tumor weight was reduced by approximately 40% compared with that of the controls. Subsequently, we found that the treatment with DIF-1 significantly decreased the phosphorylation levels of GSK-3β Ser^9 (Fig. 5B) and the protein amounts of Egr-1, TCF7L2 and cyclin D1, whereas β-catenin levels were unaltered (Fig. 5C). These results were consistent with our previous ones obtained from *in vitro* experiments using cultured HCT-116 cells, in which DIF-1 strongly inhibited HCT-116 cell proliferation by GSK-3β-mediated degradation of cyclin D1 and suppression of Egr-1 expression, which subsequently inhibited TCF7L2-mediated gene transcription without affecting β-catenin expression [27].

DIF-1 administration also significantly decreased the weight of HeLa-xenograft tumor masses (Fig. 6A). Similarly to HCT-116-xenograft tumors, the treatment with DIF-1 showed tendency to inhibit GSK-3β Ser^9 phosphorylation, although it was not statistically significant (Fig. 6B). DIF-1 treatment significantly decreased the expression of β-catenin, TCF7L2 and cyclin D1 (Fig. 6C), consistent with our previous results obtained using cultured HeLa cells [21,22], indicating that DIF-1 inhibited HeLa-xenograft tumor growth by GSK-3β-mediated degradation of cyclin D1 and suppression of the Wnt/β-catenin signaling pathway.

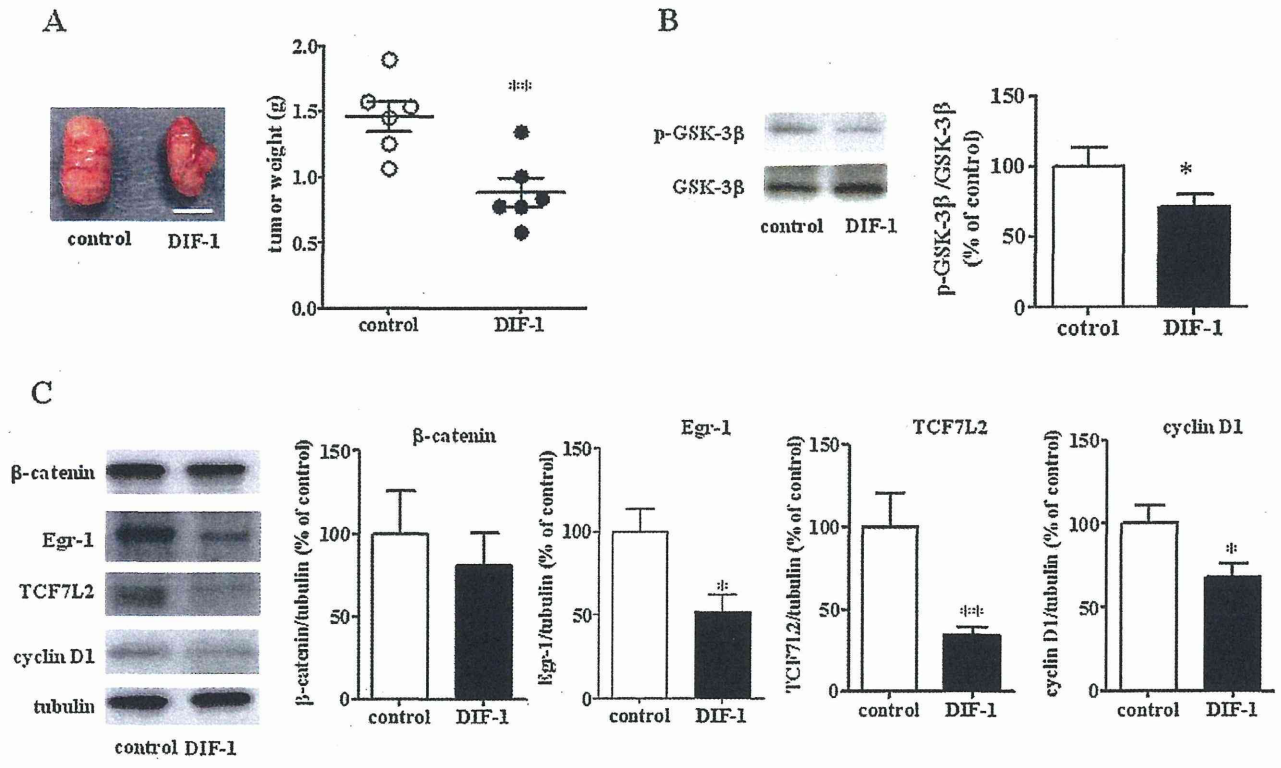

Fig. 5. Effect of orally administered DIF-1 on HCT-116-xenograft tumors.
A. Tumor appearance and weight. HCT-116 cells suspended in Matrigel were subcutaneously injected into the right flanks of mice. Tumor masses were removed after 2 weeks. Photographs show representative tumors isolated from each group of mice. Scale bar indicates 1 cm. Values are the means ± s.e.m. ($n = 6$). *$P < 0.05$ vs. control, **$P < 0.01$ vs. control (Student's *t*-test). B. GSK-3β phosphorylation levels. Protein samples were prepared from enucleated tumors and analyzed by Western blotting for phosphorylation of GSK-3β Ser^9. The membranes were stripped and then reprobed with an anti-GSK-3β antibody. Band densities are shown as percentages of the controls. Values are the means ± s.e.m. ($n = 6$). *$P < 0.05$ vs. control (Student's *t*-test). p-GSK-3β, Ser^9 phosphorylated GSK-3β. C. Expression levels of Wnt signaling-related proteins. Protein samples were prepared from enucleated tumors and analyzed by Western blotting for β-catenin, Egr-1, TCF7L2, and cyclin D1. Band densities were quantified and normalized to those of tubulin. Values are the means ± s.e.m. ($n = 6$). *$P < 0.05$ vs. control (Student's *t*-test).

Please cite this article in press as: Takahashi-Yanaga F, et al. DIF-1 inhibits tumor growth *in vivo* reducing phosphorylation of GSK-3β and expressions of cyclin D1 and TCF7L2 in cancer model mice. Biochem Pharmacol (2014), http://dx.doi.org/10.1016/j.bcp.2014.03.006

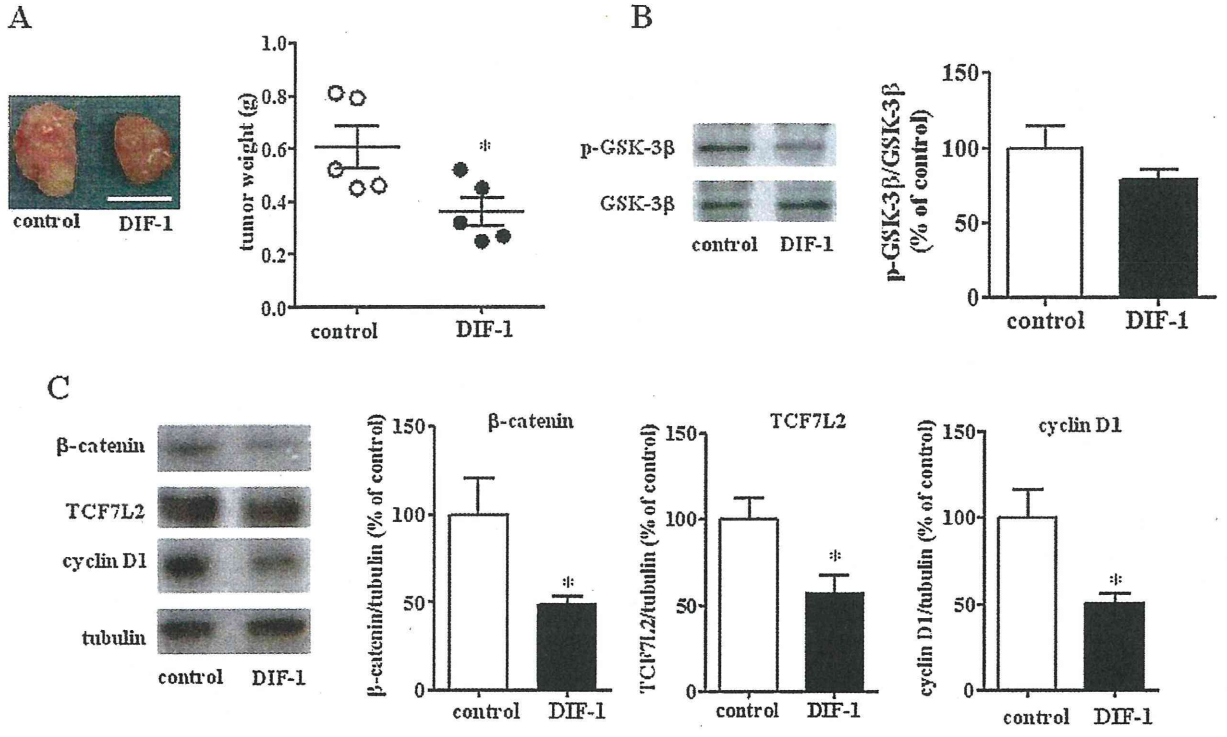

Fig. 6. Effect of orally administered DIF-1 on HeLa-xenograft tumors.
A. Tumor appearance and weight. HeLa cells suspended in Matrigel were subcutaneously injected into the right flanks of mice. Tumor masses were removed after 3 weeks. Photographs show representative tumors isolated from each group of mice. Scale bar indicates 1 cm. Values are the means ± s.e.m. ($n = 5$). *$P < 0.05$ vs. control, **$P < 0.01$ vs. control (Student's t-test). B. GSK-3β phosphorylation levels. Protein samples were prepared from enucleated tumors and analyzed by Western blotting for phosphorylation of GSK-3β Ser^9. The membranes were stripped and then reprobed with an anti-GSK-3β antibody. Band densities are shown as percentages of the controls. Values are the means ± s.e.m. ($n = 5$). *$P < 0.05$ vs. control (Student's t-test). p-GSK-3β, Ser^9 phosphorylated GSK-3β. C. Expression levels of Wnt signaling-related proteins. Protein samples were prepared from enucleated tumors and analyzed by Western blotting for β-catenin, TCF7L2, and cyclin D1. Band densities were quantified and normalized to those of tubulin. Values are the means ± s.e.m. ($n = 5$). *$P < 0.05$ vs. control (Student's t-test).

Finally, we found no significant differences in the appearance, activity, body weight, and blood cell counts between DIF-1-treated mice and the controls, despite the treatment with higher dose of DIF-1 compared with Table 1 (Fig. 7).

4. Discussion

The present study clearly showed for the first time that DIF-1 was absorbed through the digestive tract to elevate its blood concentration and inhibited *in-vivo* tumor growth without manifesting any apparent toxicity in three different cancer model animals, *Mutyh*$^{-/-}$ mice, HCT-116-bearing mice and HeLa-bearing mice, suggesting that this compound might be applicable for the treatment of human cancer. And moreover, regarding the mechanisms for the anti-tumor effect of DIF-1, we found that this compound also induced dephosphorylation of GSK-3β and reduced TCF-mediated gene transcription *in vivo*.

MUTYH is a mammalian DNA glycosylase that initiates base excision repair by excising adenine opposite 8-oxoguanine and 2-hydroxyadenine opposite guanine, thereby preventing G:C to T:A transversion mutations caused by oxidative stress [35–37]. Recently, a biallelic germline mutation of *MUTYH* has been found in humans. Those carrying this *MUTYH* mutation tend to develop multiple adenomatous colon polyps and have an increased risk of colorectal cancer in parallel with an increased incidence of G:C to T:A somatic mutations in the *APC* gene [29,30]. These mutations of the *APC* gene induce constitutive activation of Wnt/β-catenin signaling as observed in FAP patients. This type of polyposis is called MUTYH-associated polyposis (MAP). Therefore, the animal model that we employed appeared to be adequate to evaluate the clinical utility of DIF-1. The efficacy of DIF-1 for treatment of oxidative stress-induced intestinal tumors in *Mutyh*$^{-/-}$ mice was comparable with that of celecoxib, the only non-steroidal anti-inflammatory drug clinically applicable for FAP patients. Because celecoxib and DIF-1 inhibited TCF-mediated gene expression in colon cancer cells [38,39], this may be a mechanism underlying the intestinal tumor growth inhibition by DIF-1 and celecoxib.

Oral administration of DIF-1 suspended in methylcellulose inhibited tumor growth in *Mutyh*$^{-/-}$ mice, whereas at first the same treatment failed to inhibit the growth of xenograft tumors. Although we have not been able to address the precise reason for this failure, we suppose that orally administered DIF-1 might exert direct actions on tumors in the intestinal mucosa without being absorbed into systemic circulation and that the plasma concentration of DIF-1 may not have been sufficient to inhibit growth of the xenograft tumors distant from the digestive tract. It was difficult to maintain a sufficiently high plasma concentration of DIF-1 for longer than 3 h as shown in Fig. 1B. Therefore, we explored another method to improve absorption of DIF-1 and found that soybean oil was a better solvent than methylcellulose to maintain the plasma concentration of DIF-1 (Fig. 4). The reason for this may be that hydrophobic DIF-1 molecules were more soluble in oil than in water. In any case, oral administration of DIF-1 dissolved in soybean oil successfully inhibited growth of the xenograft tumors, which indicated that DIF-1 distributed through systemic circulation could inhibit tumor growth when the plasma concentration of DIF-1 was sufficiently elevated.

The phosphorylation status of GSK-3β Ser^9 indicated that DIF-1 activated or tended to activate this kinase in both *Mutyh*$^{-/-}$ mice and nude mice bearing xenograft tumors. This observation is

Please cite this article in press as: Takahashi-Yanaga F, et al. DIF-1 inhibits tumor growth *in vivo* reducing phosphorylation of GSK-3β and expressions of cyclin D1 and TCF7L2 in cancer model mice. Biochem Pharmacol (2014), http://dx.doi.org/10.1016/j.bcp.2014.03.006

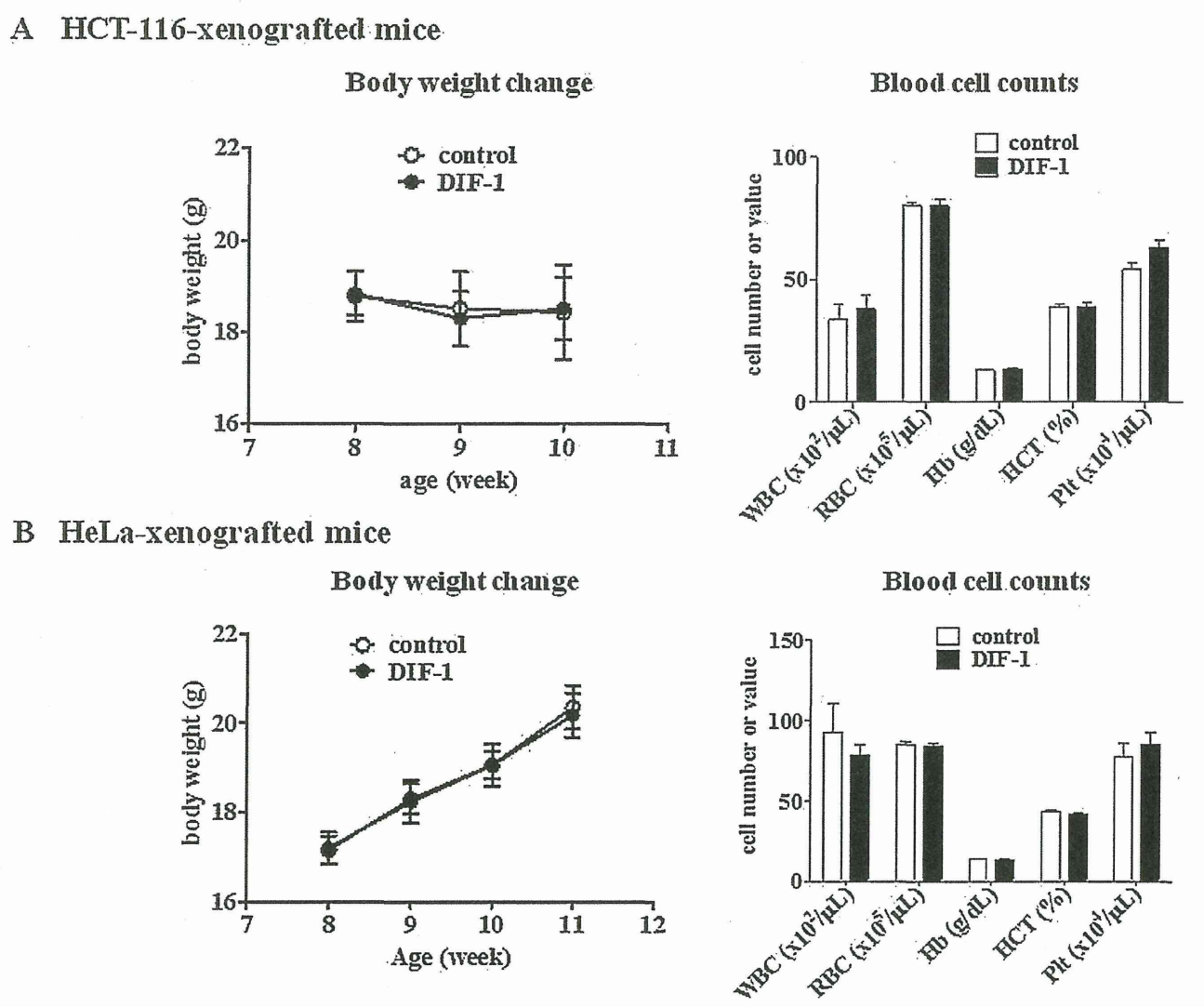

Fig. 7. Effect of DIF-1 on the body weight and blood cell counts of xenografted mice.
The body weight of xenografted mice was monitored weekly during the treatment period. Blood samples collected at the end of treatment were subjected to cell counting. A. HCT-116-xenografted mice. B. HeLa-xenografted mice. Values are the means ± s.e.m. (n = 6 for HCT-116-xenografted mice, n = 5 for HeLa-xenografted mice). WBCs, white blood cells; RBCs, red blood cells; Hb, hemoglobin; HCT, hematocrit; Plt, platelets.

consistent with our previous results obtained using cultured tumor cell lines [21–23,25,26]. Therefore, GSK-3β activiation and subsequent degradation of β-catenin may be one of important mechanisms underlying the DIF-1 action to inhibit the Wnt/β-catenin target gene expression. However, most colorectal cancers including MAP carry somatic mutations in their *APC* or *β-catenin* genes, which allow β-catenin to escape from GSK-3β-induced degradation and to accumulate in the nuclei, leading to the activation of β-catenin/TCF-mediated gene transcription [28–30]. Indeed, the β-catenin signal is constitutively activated in HCT-116 cells and probably also in the intestinal tumors developed in *Mutyh*$^{-/-}$ mice [11–14,29,30], which may be a reason why DIF-1 could not decrease β-catenin in tumors of *Mutyh*$^{-/-}$ mice and HCT-116 xenograft tumors (Figs. 3B and 5C). Despite constitutively active β-catenin, DIF-1 strongly suppressed the expression of cyclin D1 and TCF7L2 without affecting β-catenin expression levels in the intestinal tumors of *Mutyh*$^{-/-}$ mice and HCT-116-xenograft tumors. This result was consistent with our previous *in-vitro* study using HCT-116, in which we concluded that DIF-1 inhibited "Wnt target" gene expression through inhibition of Egr-1-mediated TCF7L2 gene transcription independent of β-catenin [27]. As shown in the present study, DIF-1 also suppressed the expression of Egr-1 *in vivo*, indicating that DIF-1 may inhibit tumor growth *in vivo* by the same mechanism as revealed *in vitro*.

DIF-1 may have at least three pharmaceutical merits in comparison to existing anti-cancer drugs. First, the mechanisms of its action are very unique. DIF-1 strongly inhibits the Wnt/β-catenin signaling pathway whether APC and/or β-catenin are intact or mutated, resulting in powerful suppression of the expression levels of cyclin D1 and TCF7L2. Although this pathway is often excessively activated in cancer cells, there is few anti-cancer drugs that target this pathway so far. Second, DIF-1 is unlikely to induce serious adverse reactions. DIF-1 induces cell cycle arrest at G_1 phase without affecting cell viability [21,23,25]. In the present *in-vivo* study, repeated administration of DIF-1 did not reduce the body weight or blood cell counts in mice. Certainly, it is unknown whether this cytoprotective property is advantageous in the treatment of cancer, for which cytotoxic drugs are usually used. We expect that DIF-1 is useful at least when used in combination with cytotoxic anti-cancer drugs. Third, DIF-1 can be

Please cite this article in press as: Takahashi-Yanaga F, et al. DIF-1 inhibits tumor growth *in vivo* reducing phosphorylation of GSK-3β and expressions of cyclin D1 and TCF7L2 in cancer model mice. Biochem Pharmacol (2014), http://dx.doi.org/10.1016/j.bcp.2014.03.006